High-throughput viscosity determinations

AIP | Review of Scientific Instruments

High-throughput viscosity determinations

Jing Ma, Jose M. Lopez-Pedrosa, and Mark Bradley

Citation: Rev. Sci. Instrum. **79**, 094102 (2008); doi: 10.1063/1.2976350
View online: http://dx.doi.org/10.1063/1.2976350
View Table of Contents: http://rsi.aip.org/resource/1/RSINAK/v79/i9
Published by the AIP Publishing LLC.

High-throughput viscosity determinations

Jing Ma, Jose M. Lopez-Pedrosa, and Mark Bradley[a)]
School of Chemistry, Joseph Black Building, University of Edinburgh, West Mains Road, Edinburgh EH9 3JJ, United Kingdom

(Received 21 March 2008; accepted 3 August 2008; published online 11 September 2008)

A new high-throughput viscosimeter device was designed, built, and tested allowing measurement of the viscosity of 100 different solutions in a single experiment using the falling sphere approach. Using the corrected Stokes' law, viscosities obtained by the HT device were compared to viscosities of the same solutions obtained on a conventional viscosimeter and showed excellent correlation. The theoretical set of data, correlated with Reynolds numbers, and the viscosities obtained for each sample showed very good correlation with the experimental data, demonstrating the robustness of the device. © *2008 American Institute of Physics.* [DOI: 10.1063/1.2976350]

I. INTRODUCTION

High-throughput and robotic methodologies have enabled the routine preparation and generation of large numbers of formulations in a highly efficient manner.[1–3] This ability, however, then brings to the fore the requirement to rapidly characterize the formulations that are generated, with the need to determine a range of physical parameters, which includes viscosity and density.[4] Viscosity is an especially important feature of fluids, relating to their resistance to deformation[5–7] and plays an important role in not only understanding their behavior but also dictating the possible applications any specific fluid. Experimental viscosity measurements are thus very important in many industrial areas, for example, in printing or spraying process, which require materials that fall within specific viscosity regimes in order to have practical application; and thus with high-throughput formulation generation a need arises to be able to determine the viscosity of large numbers of samples in a parallel way.

Flow regimes are classified into laminar, transitional, and turbulent flow, with the specific flow conditions distinguished by so-called Reynolds numbers (Re) a dimensionless unit proportional to [(inertial force)/(viscous force)]. When Reynolds number is small, the fluid's viscosity is dominant and, in this situation, fluid is described as being in laminar flow (and Stokes law applies). When the Reynolds number is large the fluid's inertial effects rule and turbulent flow dominates (the flow conditions between laminar flow and turbulent flow are known as transitional flow).

There are four main types of viscometers designed to measure liquid viscosity:[8–10] capillary viscometers, rotational viscosimeters, falling sphere, and vibrational viscosimeters, but the falling sphere approach has attracted attention due to simplicity of operation (the falling sphere approach allows fluid viscosity to be determined using gravitational effects and is described by Stokes' law):

$$\mu = d^2 g(\rho_1 - \rho_2)/(18V). \quad (1)$$

We, therefore, designed a novel device to characterize viscosity in an efficient high-throughput manner based on the parallelization of a falling sphere viscometer, using sphere shadow methodology as a detection approach as shown in Fig. 1. This allowed the viscosity of up to 100 Newtonian liquid compositions to be simultaneously determined by parallel measurements of the time required for a sphere to pass through the fluids.

II. EXPERIMENTAL

A. Materials

Polyvinyl chloride spheres with a diameter of 4.8 mm and a density of 1.41 g/cm^3 were purchased from Engineering Laboratories inc. Glycerol, (+99.5%, spectrophotometric grade), density: 1.263 g/cm^3 and ethylenediamine were purchased from Sigma-Aldrich.

B. Reference experiment for correction parameter determination

1 g of 4.8 mm diameter polyvinylchloride (PVC) spheres were added to 10 ml of an 80% solution of the ethylenediamine in distilled water and stirred at 80 °C for 1 h. The spheres were washed with water to remove excess ethylenediamine and dried at room temperature for 4 h.[11]

The PVC spheres were washed with glycerol and dried at room temperature for 5 min. Glycerol (5 ml) was added to a single 8 mm diameter tube and a PVC sphere was placed into a mesh hole plate, which upon withdrawing allowed the sphere to fall through the sample solution and the time for the sphere to fall from the 0 position to the 10.4 cm position was recorded.

C. High-throughput measurement of sample viscosities

The high-throughput viscosity device is depicted in Fig. 1. The system consisted of a light source, a mesh plate, an adapter mask plate, an array of holes, a base plate, and a web camera. The measuring tubes (8 mm diameter and PVC ma-

a)Author to whom correspondence should be addressed. FAX: +44 (0)131 650 6453. Tel.: +44 (0)131 650 4820. Electronic mail: mark.bradley@ed.ac.uk.

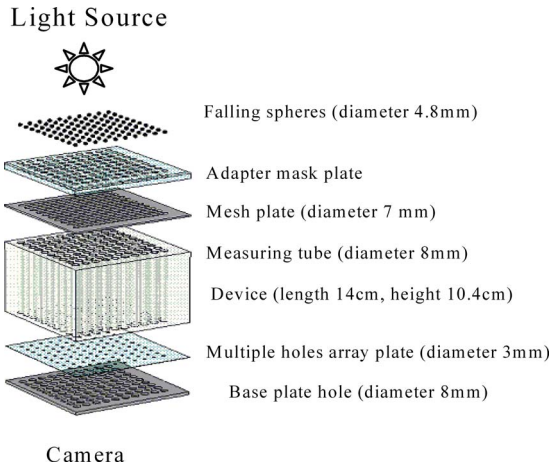

FIG. 1. (Color online) Design of the high-throughput parallel viscosity measurement device.

terial) were filled with 100 water-glycerol solutions library (shown in the Table I) and 5 ml of each sample were placed in each measurement tube of the high-throughput viscosity measurement device.

The PVC spheres were washed with the corresponding sample solutions, dried at room temperature for 10 min, placed in the mesh holes plate, and released into the solutions upon slowly withdrawing the mask plate, with the web camera triggered upon release and recording the events. When the spheres reached the holes, the holes were filled and became "dark" as is shown in Fig. 2 with a digital camera recording the images. Data processing was achieved using the methods described in elsewhere[2,3] by Image ProPlus.

D. Characterization of density and standard viscosity

The density of each sample solution was measured by a liquid density transmitter L-DENS.[1] The standard viscosity of each sample solution was measured using an automated microviscometer[1] useful for a viscosity range from 80 to 2500 mPa s and was based on the falling ball principle. This consisted of a glass capillary (4 mm diameter $\times$ 15.8 cm length with a stainless steel ball (3 mm diameter and a density of 8.75 g/ml). The measurement of dynamic viscosity was based on rolling of the ball inside the capillary at different inclination angles (from 20° to 70°). In these experiments the measurement of the viscosity was calculated taking the capillary through an inclination angle of 50° to get data comparable to the HT viscometer.

III. RESULTS AND DISCUSSION

A. Experimental, wall, and end corrections

As mentioned above Stokes' law has limitations as it is valid only for laminar flow. In reality, the true terminal velocity of the falling ball must be corrected with respect to the determined experimental velocity value. This correction for terminal velocity is due to the fact that Stokes' law works well only in fluid media with no inertial forces (when the ball moves slowly with no acceleration), no end effects (the ball falls steadily) and no wall effect (infinite Newtonian medium). In practical experiment, wall, inertial, and end effects need to be corrected for and K factors must be calculated to compensate for deviations in Stokes' law caused by experimental procedures.[12–14] In this case corrections for wall and end effects were carried out, but no corrections were necessary for the inertial effect due to the slow motion of the ball inside the measurement tube.

A reference experiment was first performed using a single tube and pure glycerol. The time needed (t=790 s) for a PVC sphere to reach the bottom of a single tube (10.4 cm long) in pure glycerol was measured and used in the corrected Stokes' Eq. (2) to calculate the experimental correction factor K_0=0.0787,

$$K = 18\ \ \mu V/d^2 g(\rho_1 - \rho_2) = 18\ \ \mu l/(d^2 g(\rho_1 - \rho_2)t). \qquad (2)$$

The second correction considered the wall effect,[15–17] being the ratio between experimental and corrected terminal velocities calculated considering the ratio d/D, using three equations:

(a) Francis equation,

$$V/Vc = K_1 = \{[1 - (d/D)]/[1 - 0.475(d/D)\ \}^4. \qquad (3)$$

(b) Ladenburg equation,

$$V/Vc = K_2 = 1/[1 + 2.1(d/D)]. \qquad (4)$$

(c) Faxen equation,

$$V/Vc = K_3 = (1 - 2.104(d/D)^3 + 2.09(d/D)^5 - 0.95(d/D)^5\ . \qquad (5)$$

The values of the K factors considering the wall effect correction are as follows: K_1=0.098, K_2=0.442, and K_3=0.115.

The third correction considered the end effect.[18] This was calculated considering various distances (h) of the ball with respect to the bottom of the tube, to ascertain the constant velocity nature of the ball falling into the tube. Values of h close to zero were studied: 0.0002, 0.00025, 0.0003, and 0.0004 m (the tube was 0.104 m). The equation for the end effect is as follows:[15,18]

$$V/Vc = [1 + (9/8)d/(2h)]^{-1} = K. \qquad (6)$$

Four values of K were determined as a function of h: K_4=0.0689 (h=0.0002); K_5=0.0847 (h=0.00025); K_6=0.1 (h=0.0003); K_7=0.129 (h=0.0004).

B. High-throughput measurement of viscosities

The traveling time of a PVC sphere going through the sample solution was recorded by a web camera with each "hole" representing a sample solution. From Fig. 2 it can be seen, at the beginning, that all the holes were empty (the holes were bright), 100 s later, some holes were filled with spheres and became dark, and the number of dark holes increased with time. At 808 s all the holes were filled with spheres and became dark as shown in Fig. 2. Using this approach the time of the fall in each well was obtained and based on the corrected Stokes' law equation as follows:

TABLE I. Composition of samples used in the HT device and the standard viscosimeter.

Entry	Glycerol (g)	Water (g)	Entry	Glycerol (g)	Water (g)
1	17	3	51	19.1	0.94
2	17.1	2.91	52	19.1	0.9
3	17.2	2.81	53	19.1	0.91
4	17.3	2.7	54	19.1	0.84
5	17.4	2.61	55	19.2	0.91
6	17.5	2.51	56	19.2	0.82
7	17.6	2.41	57	19.2	0.81
8	17.7	2.3	58	19.2	0.78
9	17.8	2.2	59	19.2	0.76
10	17.9	2.08	60	19.3	0.84
11	18	2	61	19.3	0.66
12	18.1	1.91	62	19.3	0.72
13	18.2	1.76	63	19.3	0.7
14	18.2	1.8	64	19.3	0.68
15	18.2	1.76	65	19.3	0.74
16	18.2	1.81	66	19.4	0.62
17	18.2	1.85	67	19.4	0.61
18	18.3	1.75	68	19.4	0.61
19	18.3	1.74	69	19.4	0.58
20	18.3	1.72	70	19.5	0.54
21	18.3	1.7	71	19.5	0.54
22	18.4	1.63	72	19.5	0.52
23	18.4	1.65	73	19.5	0.5
24	18.4	1.64	74	19.5	0.48
25	18.4	1.6	75	19.5	0.46
26	18.4	1.57	76	19.6	0.44
27	18.5	1.53	77	19.6	0.42
28	18.5	1.5	78	19.6	0.39
29	18.5	1.45	79	19.6	0.38
30	18.6	1.42	80	19.6	0.36
31	18.6	1.36	81	19.7	0.3
32	18.7	1.29	82	19.7	0.28
33	18.7	1.27	83	19.7	0.26
34	18.7	1.27	84	19.7	0.34
35	18.7	1.35	85	19.7	0.32
36	18.7	1.32	86	19.8	0.24
37	18.8	1.16	87	19.8	0.22
38	18.8	1.24	88	19.8	0.21
39	18.8	1.22	89	19.8	0.18
40	18.8	1.2	90	19.8	0.16
41	18.8	1.18	91	19.9	1.08
42	18.9	1.14	92	19.9	0.14
43	18.9	1.09	93	19.9	0.12
44	18.9	1.08	94	19.9	0.1
45	18.9	1.13	95	19.9	0.08
46	18.9	1.09	96	19.9	0.06
47	19	1.05	97	20	0.02
48	19	0.97	98	20	0.04
49	19	0.96	99	20	0
50	19	1.02	100	20.1	1.09

$$\mu = K_n d^2 g(\rho_1 - \rho_2)/(18V_c). \quad (7)$$

In order to study the performance of the high-throughput viscosity measurement device the viscosity of 100 samples were determined using both the HT device and a conventional automated viscosimeter. Corrections of terminal velocity V_C (considering experimental, wall, and end effects) were

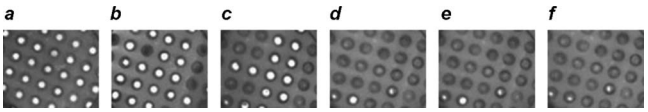

FIG. 2. Sphere shadow pictures. (a) $t=0$ s, (b) $t=100$ s, (c) $t=300$ s, (d) $t=650$ s position, (e) $t=750$ s, and (f) $t=808$ s.

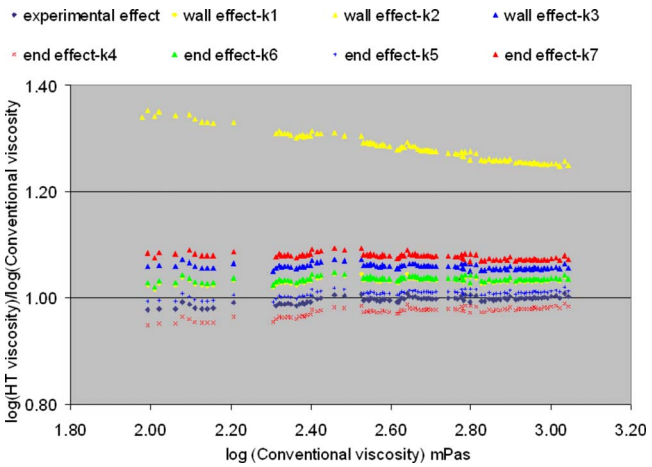

FIG. 3. (Color online) Viscosity correlation between data obtained using the high-throughput parallel method developed here (HT viscosity with experimental, wall, and end effect corrections; see Sec. III A for details) and those determined on a one-by-one basis using a conventional automated microviscometer. Regression coefficient (R^2) is 0.996.

calculated for the HT values and correlations between these data and conventional viscosity data were carried out, as shown in Fig. 3.

Figure 3 shows the correlation between conventional viscosity data and the data obtained with the HT viscometer device (with experimental, end, and wall corrections). It can be said that most of the lines were very closed each other and showed excellent correlation with the conventional viscosity data. As expected the wall effect correction constant from Francis' equation (K_1) worked very well as in this case d/D is equal to 0.6 which is within the range of Francis' equation[15] ($d/D<0.9$) ($K_1=0.098$ very close to the experimental correction factor $K_0=0.079$). On the other hand the viscosity data using Ladenburg's constant (K_2) showed the biggest discrepancy as the d/D values should be lower than 0.1 for this equation to apply.

Experimental final velocities were calculated using the correction factors (K_0-K_7) and using the following equations:

$$V\exp = L/t, \tag{8}$$

$$Vc = V\exp/K_n. \tag{9}$$

Reynolds numbers were taken in the range from 0.01 to 1.55 and were introduced into the Eqs. (10) and (11) to determine theoretical viscosity and theoretical terminal velocity.

$$\mu = [(4r^3 g(\rho_1 - \rho_2)\rho_2)/(9\ \mathrm{Re})]^{1/2}, \tag{10}$$

$$V = (\mathrm{Re}\ \mu)/(d\rho_2). \tag{11}$$

The corrected experimental velocities (with different K_n values) were compared to the theoretical terminal velocities as shown in the Fig. 4.

Figure 4 shows that the terminal velocities of the samples determined with the HT viscometer increased as the time of the fall of the ball increases.

It can be seen that long fall times (100–1000 s) at all the terminal velocities were very close, suggesting high sample viscosity and low Reynolds number and low deviation from Stokes' law. Theoretical velocity values estimated with low values of Reynolds numbers were very close to the corrected terminal velocities corresponding to the wall effect corrections (K_1), end effect (K_6) and the experimental correction factor (K_0).

Reynolds numbers for the HT viscometer were also calculated using

$$\mathrm{Re} = 2\rho_2 rV/\mu = 4r^3\rho_2(\rho_1 - \rho_2)g/9\mu^2. \tag{12}$$

Figure 5 shows that there is a dramatic deviation of the Reynolds numbers of the samples from both devices; however, the viscosity values are very similar in both cases due to the corresponding correction constants. It can be said that for low Reynolds number values in the range from 0.1 to 0.01, the majority of the samples in both devices coincides, because the viscosity values in both of them are higher and thus Stokes' law complies very well. On the other hand there are deviations in both devices when the Reynolds numbers are in the range from 0.1 to 0.5, due to the low viscosity of the samples as well as the physical parameters of each device such as spheres (size and density), the lengths and diameters of the capillary (conventional viscometer) and tubes (HT).

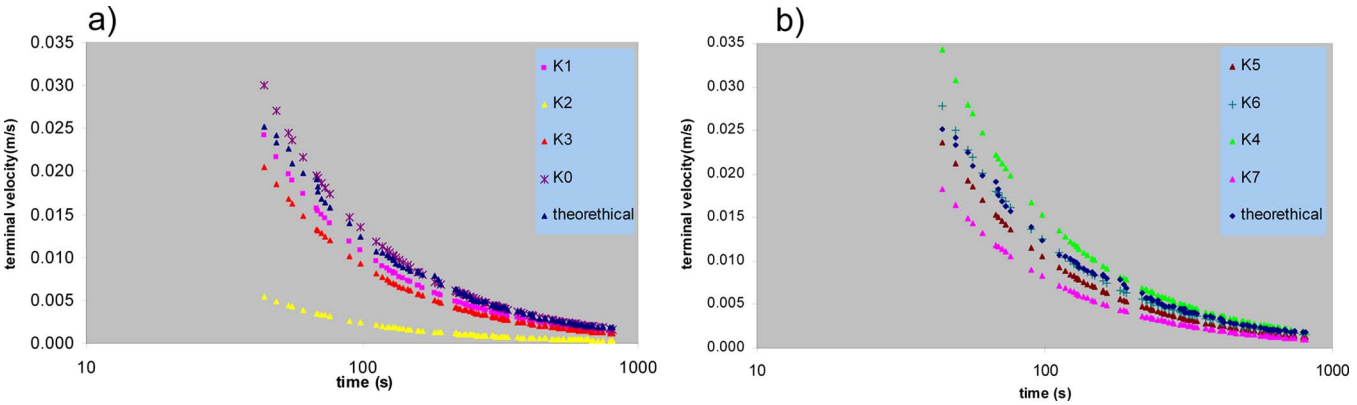

FIG. 4. (Color online) Comparison of the calculated experimental velocities (with different K_n values) with the theoretical terminal velocities.

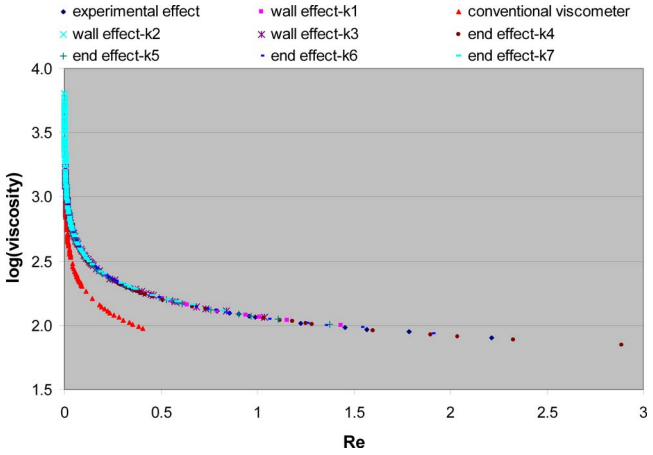

FIG. 5. (Color online) The performance of the high-throughput viscometer measurement device with various correction factors and calculated Reynolds numbers.

C. Statistical treatment

Statistical analysis based on both descriptive analysis and viscosity values comparisons were carried out. Descriptive analysis allowed determination of the main statistical descriptors for each viscosity data set determined for each correction factor (K_0 and K_5) and for the standard viscometer. Test analyses were carried out by analysis of the correction factors determined from the high-throughput viscometer and those determined using the standard viscometer. Despite the many correction factors determined, those with the best fit with the viscosity values of the standard viscometer were chosen, with two correction factors K_0 (experimental) and K_5 (end effect for $z=0.00025$) selected.

1. Descriptive analysis

This was carried out by considering an analysis of the distribution of each population of viscosity values, determined individually, for each correction factor with the standard viscometer. This analysis was based on the study of cumulative frequency, which gives the values of the viscosity population for a given value of percentage, considering 100% of the population. Analysis of the data distribution was carried out as shown in the Table II.

Table II shows that the data distribution was not symmetric with a skew to the right. It was found that when comparing, both the mean and the standard error of the standard viscometer with the HT viscometer (K_0), their values were nearly identical, however, there was more variation in the case of the standard viscometer when compared to the HT viscometer, with a K_5 value of 6.32% for the mean and 8.85% for the standard error.

TABLE II. Statistical descriptors of the viscosity data distribution.

Statistical descriptor	Standard viscometer (mPa s)	HT viscometer (correction factor: K_0) (mPa s)	HT Viscometer (correction factor: K_5) (mPa s)
Mean	489	485	522
Standard error	27.8	28.3	30.5
Percentile: 10%	138	125	134
Percentile: 25%	245	234	252
Percentile: 50%	439	451	486
Percentile: 75%	687	666	717
Data range	1008	1071	1153
Interpercentile	442	432	465

For lower values of the percentile (10% to 25%), the data distribution showed viscosity values were virtually identical for the standard and the HT viscometer (K_5). The data distributions were indeed similar for the case of the standard viscometer and the HT viscometer (K_0), for percentile values equal or greater than the median values.

Confidence intervals from the HT and the standard viscometers were determined as shown in Table III.

TABLE III. Confidence intervals for the HT and the standard viscometers.

Data distribution (%)	HT viscometer (correction factor: K_0) (mPa s)	HT viscometer (correction factor: K_5) (mPa s)	Standard viscometer (mPa s)
95	485 ± 56	522 ± 60	489 ± 55
99	485 ± 73	522 ± 79	489 ± 72

2. Viscosity value comparison: Test analysis[19]

The compaison was carried out comparing the results of the standard viscometer (reference) and the HT viscometer, using two factor corrections: K_0 (experimental) and K_5 (end effect for $z=0.00\ 025$) as follows.

Partial least square analysis. In this case correlation analysis was carried out to check the fit of both correction factors with the standards, with analysis carried out using linear regression, using

$$y = a + bx. \tag{12'}$$

The partial least-squares analysis gave the main parameters as shown in Table IV.

Table IV shows that there was good correlation between the two correction factors (slope b were very similar, with only approximately 7% of variation), while their intercepts (a), had only 5.7% variation. However the standard error of the estimate (S_{YX}) of the regression was higher in the case of the comparison with the correction factor (K_5) than the comparison of the correction factor (K_0) (approximately 8.6% of variation).

Fisher distribution-test. A Fisher distribution-test (F-test) was used with the aim at comparing the variance of two populations using a one-tailed test for $p=0.05$. This comparison was carried out by determining the F ratio of the two populations as shown in expression (13) and comparing the ratio with a critical value of the Fisher distribution ($F_c = 1.394$) for a distribution with 95% and 99% degrees of

TABLE IV. Main parameters of the PLS analysis.

Viscosity comparison between HT correction factors and Standard	a	b	r^2	S_{YX}
Correction factor (K_0) vs standard	−12.69	1.0191	0.9975	14.0
Correction factor (K_5) vs standard	−13.45	1.0964	0.9975	15.31

TABLE V. *F*-test values.

Viscosity comparison between the correction factors of HT and standard	*F*	*p*
Correction factor (K_0) vs standard	1.041	0.420
Correction factor (K_5) vs standard	1.205	0.177

freedom (ν).

If the variance of the population $1[\sigma^2(1)]$ is similar to the population $2[\sigma^2(2)]$ and $F<F_c$, then the two populations have the same variance.

$$F = \sigma^2(1)^* \nu_2 / \sigma^2(2)^* \nu_1. \quad (13)$$

In this case, comparison of the viscosity data set for the two factor corrections (K_0 and K_5) with the viscosity values of the standard viscometer was carried out looking at the *F* ratio of variance, considering a 5% confidence level ($p=0.05$), and a one tail distribution.

Table V shows the values of *F* determined for the viscosity values of the HT method for each correction factor and the viscosity values for the standard viscometer:

Table V shows that $F<Fc$ for both correction factors. Furthermore their *p* values were greater than $p=0.05$, and so the viscosity values determined by the HT method, for both correction factors (K_0 and K_5) were not significantly different compared to those determined by the standard viscometer.

Moreover it can be said that the viscosity values of the two correction factors (K_0 and K_5) were precise, with viscosity value of K_0 being more precise than those belong to K_5 .

z Test. This test shows whether the sample mean and the population mean between the two populations is statistically significant. Therefore for $z>z_c$ the values of the comparison of the sample mean (chosen randomly) with the population mean were significant at $p=0.05$. Therefore the comparison of the HT viscosity values of the correction factors (K_0 and K_5) and the standard viscosity values was carried out considering expression (14), for a $z_c=1.645$ and for $p=0.05$.

$$z = [(X_{\mathrm{HT}}\text{-}X_s) - (\mu_{\mathrm{HT}}\text{-}\mu_S)]/(\sigma^2_{\mathrm{HT}}/N_{\mathrm{HT}} + \sigma^2_s/N^{1/2}_s). \quad (14)$$

In this *z* test, ten samples were chosen randomly from each population of the viscosity for each correction factor (K_0 and K_5) and the sample mean difference between each correction factor of the HT (X_{HT}) with the Standard (X_S) analyzed to see if it complied with the expressions of the null hypothesis (H_0) (15) or the alternative hypothesis (H_1) (16).

$$H_{0:}\ (X_{\mathrm{HT}}\text{-}X_S) \leq 150 \quad \text{(sample mean difference no significant at } p=0.05), \quad (15)$$

$$H_{1:}\ (X_{\mathrm{HT}}\text{-}X_S) > 150 \quad \text{(sample mean difference significant at } p=0.05). \quad (16)$$

The values of these sample mean differences (X_{HT}-X_S) were higher than the values of the difference of the population mean (μ_{HT}-μ_S), being −3.5 mPa s for the case of the correction factor (K_0) and 33.7 mPa s for the case of the correction factor (K_5), respectively. For each correction factor (K_0 and K_5) of the HT viscometer and its comparison with the standard viscometer the following results (Table VI) were generated.

Table VI shows that the higher the sample mean difference between the correction factors of the HT and the standard viscometers the higher the *z* values were and so the differences between the sample means were significant. Therefore it can be said that for sample mean difference ≤150 mPa s, the difference between the viscosity values of the correction factors and the standard viscosimeter was not significant and $z<z_c$, complying with the null hypothesis.

TABLE VI. *z* -test values for the method and reference comparison.

Sample mean difference X_{HT}-X_S	*z*-value HT-(K_0): standard	*p*-value HT-(K_0): standard	*z* -value HT-(K_5): standard	*p*-value HT-(K_5): standard
100	0.82	0.206	0.51	0.305
150	1.22	0.110	0.89	0.187
200	1.62	0.053	1.27	0.102
250	2.02	0.022	1.66	0.048

On the other hand for the correction factors with viscosity values of 250 mPa s more than the viscosity values of the standard viscometer, the difference was significant because the probability (*p* values) was very low and <0.05.

IV. CONCLUSIONS

A high-throughput viscosity measurement device was fabricated based on the principle of a falling sphere viscometer and assisted sphere shadow methodology. A series of 100 glycerol/water fluids was used to test and validate the high-throughput viscosity measurement device in comparison to a traditional viscometer. The results demonstrated that the high-throughput viscosity measurement device worked exceptionally well under low Reynolds number flow conditions, and that this device could be considered as an easy to use and low cost novel measurement device. The one limitation was that because light must pass though the fluids, the device is limited to physically similar transparent solutions.

Statistical treatment showed a slightly skewed trend, but the data distribution was similar to the standard viscometer with similar standard errors. Partial least-squares (PLS) analysis gave good correlation coefficients, while *F* and *z* tests showed precision and accuracy in the comparison of the correction factors (K_0 and K_5) from the HT and standard viscometers.

V. Supplemental material available

Supplemental tables with the determination of density, viscosity, Reynolds numbers of the 100 samples, and the velocity of the ball inside the device, for both the HT and the standard viscosimeter devices are available, as well as the data for the theoretical values of Reynolds number, viscosity, and velocity.

ACKNOWLEDGMENTS

The authors thank the EPSRC-GB for funding.

NOMENCLATURE

d = ball diameter (m)
D = tube diameter (m)
L = tube length (m)
t = falling time (s)
V_{exp} = experimental velocity (m/s)
V_c = corrected velocity (m/s)
V = theoretical velocity (m/s)
μ = viscosity (mPa s)
ρ_1 = ball density (kg/m)
ρ_2 = sample density (kg/m)
g = gravity acceleration (9.8 m/s^2)
Re = Reynolds number
r = ball radius (m)
h = distance of the ball from the bottom (m)
K_n = correction constant for $n=0-7$
a = intercept
b = slope
r^2 = correlation coefficient
S_{YX} = standard error of estimate
X_{HT} = viscosity mean value of the chosen ten samples from the HT viscometer
X_S = viscosity mean values of the chosen ten samples from the standard viscometer
μ_{HT} = viscosity mean value of the population of the HT viscometer
μ_S = viscosity mean value of the population of the Standard viscometer
p = level of significance
ν_1 = freedom degree of population 1
ν_2 = freedom degree of population 2
σ^2_{HT} = variance of the viscosity values of the HT viscometer
σ^2_S = variance of the viscosity values of the standard viscometer
N_{HT} = number of observations of the population belong to the HT viscometer
N_s = number of observations of the population belong to the standard viscometer

[1] J. M. Pedrosa and M. Bradley, Pigment and Resin Technology **37**, 131 (2008).
[2] T. Cull, M. Goulding, and M. Bradley, Adv. Mater. (Weinheim, Ger.) **19**, 2355 (2007).
[3] T. Cull, M. Goulding, and M. Bradley, Rev. Sci. Instrum. **76**, 062216 (2005).
[4] A. M. F. Palavra, M. A. Cardoso, J. A. P. Coelho, and M. F. B. Mourato, Chem. Eng. Technol. **30**, 689 (2007).
[5] T. Kinugasa, A. Kondo, S. Nishimura, Y. Miyauchi, Y. Nnishii, K. Watanabe, and H. Takeuchi, Colloids Surf., A **204**, 193 (2002).
[6] R. Lundstrum, A. R. H. Goodwin, K. Hsu, M. Frels, D. R. Caudwell, J. P. M. Trusler, and K. N. Marsh, J. Chem. Eng. Data **50**, 1377 (2005).
[7] K. A. Dadd and N. A. Van Wagoner, J. Volcanol. Geotherm. Res. **114**, 63 (2002).
[8] M. J. C. Flude and J. E. Daborn, J. Phys. E **15**, 1313 (1982).
[9] D. I. Atkins and J. S. Ervin, Energy Fuels **19**, 1935 (2005).
[10] A. M. J. Davis and H. Brenner, Phys. Fluids **13**, 3086 (2001).
[11] B. Balakrishnan and A. Jayakrishnan, Trends Biomater., Artif. Organs **18**, 230 (2005).
[12] E. Bar-Ziv, B. Zhao, E. Mograbi, K. David, and G. Ziskind, Phys. Fluids **14**, 2015 (2002).
[13] V. Dolejs, P. Dolecek, and B. Siska, Chem. Eng. Process. **37**, 189 (1998).
[14] A. M. Lali, A. S. Khare, J. B. Joshi, and K. D. P. Nigam, Powder Technol. **57**, 39 (1989).
[15] V. Fidleris and R. L. Whitmore, Br. J. Appl. Phys. **12**, 490 (1961).
[16] D. D. Atapattu, R. P. Chhabra, and P. H. T. Uhlherr, J. Non-Newtonian Fluid Mech. **38**, 31 (1990).
[17] J. L. Sutterby, Trans. Soc. Rheol. **17**, 559 (1973).
[18] J. L. Sutterby, Trans. Soc. Rheol. **17**, 575 (1973).
[19] J. O. Westgard and M. R. Hunt, Clin. Chem. **19**, 1 (1973).